Comparative Regge analysis of Λ, Σ^0, $\Lambda(1520)$ and Θ^+ production in γp, πp and pp reactions

V.Yu. Grishina[1], L.A. Kondratyuk[2], W. Cassing[3,a], M. Mirazita[4], and P. Rossi[4]

[1] Institute for Nuclear Research, 60th October Anniversary Prospect 7A, 117312 Moscow, Russia
[2] Institute for Theoretical and Experimental Physics, B. Cheremushkinskaya 25, 117218 Moscow, Russia
[3] Institute for Theoretical Physics, University of Giessen, Heinrich-Buff-Ring 16, D-35392 Giessen, Germany
[4] INFN - Laboratori Nazionali di Frascati, CP 13, Via E. Fermi, 40, I-00044 Frascati (RM), Italy

Abstract. Using the Quark-Gluon Strings Model —combined with Regge phenomenology— we perform a comparative analysis of Λ, Σ^0, $\Lambda(1520)$ and Θ^+ production in binary reactions induced by photon, pion and proton beams on the nucleon. We find that the existing experimental data on the $\gamma p \to K^+ \Lambda$ differential and total cross-sections can be described very well by the model for photon energies 1–16 GeV and $-t < 2$ GeV^2 assuming a dominant contribution of the K^* Regge trajectory. Moreover, using the same parameters we also reproduce the total $\gamma p \to K^+ \Sigma^0$ and $\gamma p \to K^+ \Lambda(1520)$ cross-sections suggesting a "universality" of the Regge model. In order to check the consistency of the approach we evaluate the differential and total cross-sections for the reaction $\pi^- p \to K^0 \Lambda$ which is also found to be dominated by the K^* Regge trajectory. Using the apparent "universality" of the Regge model we extend our scheme to the analysis of the binary reactions $\gamma p \to \bar{K}^0 \Theta^+$, $\pi^- p \to K^- \Theta^+$ and $pp \to \Sigma^+ \Theta^+$ as well as the exclusive and inclusive Θ^+ production in the reactions $pp \to p\bar{K}^0 \Theta^+$ and $pp \to \Theta^+ X$. Our detailed studies demonstrate that Θ^+ production does not follow the "universality" principle, thus suggesting an essentially different internal structure of the exotic baryon relative to conventional hyperons or hyperon resonances.

PACS. 13.75.Gx Pion-baryon interactions – 13.75.Jz Kaon-baryon interactions – 12.39.Mk Glueball and nonstandard multi-quark/gluon states

1 Introduction

In spite of the belief that the structure of baryons in the octet and decuplet representation is roughly understood (and exhausted), recent claims on the discovery of the manifestly exotic baryon Θ^+ have opened a new chapter in hadron physics (see, *e.g.*, refs. [1–11]). Although the existence and properties of this exotic and long-lived baryonic state still need final experimental confirmation, a variety of theoretical models have been set up with different assumptions about the internal structure of the Θ^+. Here the quark-soliton model of Diakonov, Petrov and Polyakov [12] was the first to claim the existence of an antidecuplet with rather narrow spectral width (actually prior to the experimental observations). However, the Θ^+ might also be "bound" due to strong diquark correlations (in a relative p-wave) as proposed in ref. [13] or due to a strong mixing with the octet [14]. Alternatively, it might even be explained on the basis of the constituent-quark

model involving clusters [15]. Further models have been proposed in the last 2 years, which all claim a different dynamical origin of the pentaquark Θ^+ [16,17] (cf. [18] and references cited therein). Additionally, the properties of the exotic state have been analysed within the framework of QCD sum rules [19] and even lattice QCD [20–23].

However, for a better understanding of this exotic state and its wave function (in terms of the elementary degrees of freedom) it is very important to study the dynamics of Θ^+ production in comparison to the production of non-exotic strange baryons. In this respect exclusive reactions with strangeness ($s\bar{s}$) production are of interest, *i.e.* (starting with γ-induced reactions)

$$\gamma p \to \bar{K}^0 \Theta^+ , \qquad (1)$$

$$\gamma p \to \bar{K}^{*0} \Theta^+ \qquad (2)$$

and

$$\gamma d \to \Lambda \Theta^+ . \qquad (3)$$

The first two reactions (1) and (2) —where the s-quark ends up in the mesonic final state— can be compared with

a e-mail: Wolfgang.Cassing@theo.physik.uni-giessen.de

Λ production in the binary reactions

$$\gamma p \rightarrow K^+ \Lambda, \tag{4}$$

$$\gamma p \rightarrow K^{*+} \Lambda, \tag{5}$$

where the s-quark ends up in the hyperon. Note that very detailed measurements of reaction (4) have been performed in the energy range from threshold up to a photon energy of 2.6 GeV [24]. The third reaction (3), furthermore, can be compared with the two-body deuteron photodisintegration reaction $\gamma d \rightarrow pn$ which has been studied recently at Jlab [25].

We recall that several studies of Θ^+ photoproduction have been performed within the framework of isobar models using the Born approximation [26–31]. Since these models involve a variety of uncertain parameters (coupling constants and cutoffs), the resulting cross-sections differ from several nb to almost 1 μb. On the other hand, the Regge model has a substantial advantage that the amount of uncertain parameters is much lower and that the latter can be fixed by other reactions in a more reliable fashion [32]. Accordingly, in this work we will apply the Quark-Gluon Strings Model (QGSM) combined with Regge phenomenology to the analysis of the differential and total cross-sections of the exclusive reactions $\gamma p \rightarrow K^+ \Lambda$, $\gamma p \rightarrow K^+ \Sigma^0$ and $\gamma p \rightarrow \bar{K}^0 \Theta^+$. Similar final channels will be investigated also for pion- and proton-induced reactions.

We note that the QGSM was originally proposed by Kaidalov in ref. [33] for the description of binary hadronic reactions; as demonstrated in refs. [33,34], the QGSM describes rather well the experimental data on exclusive and inclusive hadronic reactions at high energy. More recently, this model has been also successfully applied to the description of the nucleon and pion electromagnetic form factors [35] as well as of the deuteron photodisintegration [25,36,37].

We recall that the QGSM is based on two ingredients: i) a topological expansion in QCD and ii) the space-time picture of the interactions between hadrons, that takes into account the confinement of quarks. The $1/N$ expansion in QCD (where N is the number of colors N_c or flavors N_f) was proposed by 't Hooft [38]; the behavior of different quark-gluon graphs according to their topology, furthermore, was analyzed by Veneziano [39] with the result that in the large N limit the planar quark-gluon graphs become dominant. This approach —based on the $1/N_f$ expansion [39] with $N_c \sim N_f$— was used by Kaidalov [33, 34] in formulating the QGSM. Again, for sufficiently large N_f, the simplest planar quark-gluon graphs were found to give the dominant contribution to the amplitudes of binary hadronic reactions. Moreover, it can be shown that (in the space-time representation) the dynamics described by planar graphs corresponds to the formation and break-up of a quark-gluon string (or color tube) in the s-channel (see, e.g., [40–44]). On the other hand, an exchange of the u and $\bar{s}$ quarks in the t-channel implies that the energy behavior of the amplitudes —described by quark diagrams in fig. 1— is given by the contribution of the K^* Regge trajectory. In this sense the QGSM can be considered as
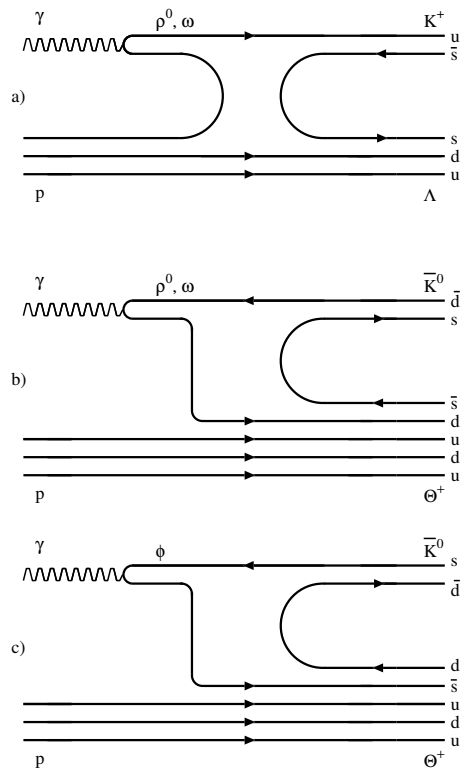

Fig. 1. Quark planar diagrams describing the binary reactions: $\gamma p \rightarrow K^+ \Lambda$ (a), $\gamma p \rightarrow \bar{K}^0 \Theta^+$ (b and c).

a microscopic model of Regge phenomenology. This, in turn, allows to obtain many relations between amplitudes of different binary reactions and residues of Regge poles which determine these amplitudes [33,34,45].

Our investigation is organized as follows: In sect. 2 we outline our approach and present the results for the differential cross-sections $\gamma p \rightarrow K^+ \Lambda$, $K^+ \Sigma^0$, $\bar{K}^0 \Theta^+$. In sect. 3 we compare total cross-sections for the reactions $\gamma p \rightarrow K^+ \Lambda(1520)$ and $\gamma p \rightarrow \bar{K}^0 \Theta^+$, while in sect. 4 we step on with the pion-induced reactions $\pi^- p \rightarrow K^0 \Lambda$ and $\pi^- p \rightarrow K^- \Theta^+$. An analysis of Θ^+ production in exclusive and inclusive NN collisions is presented in sect. 5, while a summary of our studies is given in sect. 6.

2 The reactions $\gamma p \rightarrow K^+ \Lambda$, $\gamma p \rightarrow K^+ \Sigma^0$ and $\gamma p \rightarrow \bar{K}^0 \Theta^+$

We first concentrate on γ-induced reactions and work out the Regge model in more detail. The reaction $\gamma p \rightarrow K^+ \Lambda$ can be described by the exchange of two valence (u and $\bar{s}$) quarks in the t-channel with any number of gluon exchanges between them (fig. 1a)). Alternatively, in terms of the Regge phenomenology this diagram corresponds to the K^*-Reggeon exchange mechanism shown in fig. 2a).
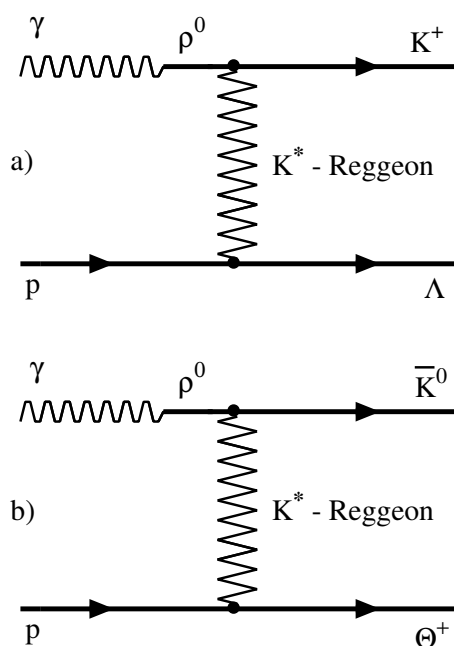
Fig. 2. K^*-Reggeon exchanges corresponding to the quark planar diagrams of fig. 1.

Employing the Regge model further on, we can write the $\gamma p \to K^+ \Lambda$ amplitude in the form

$$T(\gamma p \to K^+ \Lambda) \simeq \frac{e}{2\gamma_\rho} T(\rho^0 p \to K^+ \Lambda) =$$

$$\frac{e}{2\gamma_\rho} g_{\rho K K^*} g_{p K^* \Lambda} F_1(t) (-s/s_0^{K\Lambda})^{\alpha_{K^*}(t)} . \qquad (6)$$

Here $e^2/4\pi$ is the fine-structure constant, $\gamma_\rho^2/4\pi = 0.55$, $\alpha_{K^*}(t)$ is the K^* Regge trajectory, $s_0^{K\Lambda} = (M_\Lambda + m_K)^2$, $g_{\rho K K^*}$ and $g_{p K^* \Lambda}$ are the coupling constants describing the interaction of the K^*-Reggeon with the ρK and $p\Lambda$ systems. Within the Reggeized-Born-term model (see, *e.g.*, refs. [46–48]) it is assumed that the coupling constants g_i in the Regge amplitude of eq. (6) can be identified with the coupling constants in an effective Lagrangian model. However, it is difficult to justify this assumption and we do not address this model here. We follow another approach for a "Reggeization of the amplitude" as proposed in refs. [35–37], *i.e.* by using the s-channel convolution representation in the QGSM. In this approach one can express the amplitude for the reaction $\gamma p \to K^+ \Lambda$ in terms of the s-channel convolution of two amplitudes: $T(\gamma p \to q + qq)$ and $T(q + qq \to K^+ \Lambda)$ (see fig. 1). Then —using the Regge representation for the hadron-quark and quark-hadron transition amplitudes— we can Reggeize the binary amplitude $\gamma p \to K^+ \Lambda$. Such a procedure was applied in refs. [36,37] to define the spin structure of the deuteron photoproduction amplitude. We point out that this approach is more general and gives a vertex structure of the amplitude at negative t different from the Reggeized Born term.

Assuming, furthermore, that the Θ^+ is a pentaquark of structure $(uudd\bar{s})$, we can use a similar strategy for the

$\gamma p \to \bar{K}^0 \Theta^+$ reaction. The relevant quark diagrams for this reaction are shown in fig. 1b), c). It is obvious that in terms of the Regge phenomenology we can also use the K^*-Reggeon exchange model to describe the reaction $\gamma p \to \bar{K}^0 \Theta^+$ (cf. fig. 2b)). The $\gamma p \to \bar{K}^0 \Theta^+$ amplitude reads, accordingly,

$$T(\gamma p \to \bar{K}^0 \Theta^+) \simeq \frac{e}{2\gamma_\rho} T(\rho_0 p \to \bar{K}^0 \Theta^+) =$$

$$\frac{e}{2\gamma_\rho} g_{\rho K K^*} g_{p K^* \Theta} F_2(t) (-s/s_0^{K\Theta})^{\alpha_{K^*}(t)} \qquad (7)$$

with $s_0^{K\Theta} = (M_\Theta + m_K)^2$. In the following calculations the form factor squared $|F_i|^2$ in (6), (7) is chosen always in the form

$$|F_i|^2 = (1 - B_i t) \exp(2R_i^2 t). \qquad (8)$$

For the further developments it is important to recall that the QGSM originally was formulated for small scattering angles (or small negative 4-momentum transfer (squared) $-t$). Thus, the question arises about the extrapolation of the QGSM amplitudes to large angles (or large $-t$). Here we adopt the same concept as in our previous works [36,37]: following Coon *et al.* [49] we assume that only a single analytic Regge term with a logarithmic trajectory gives the dominant contribution to large-momentum-transfer processes. As shown in [49], such a model (denoted as "logarithmic dual model") can describe very well the differential cross-section $d\sigma/dt$ for elastic pp scattering in the energy range of 5–24 GeV/c for $-t$ up to 18 GeV^2. The logarithmic Regge trajectory itself can be written in the form

$$\alpha(t) = \alpha(0) - (\gamma\nu)\ln(1 - t/T_B). \qquad (9)$$

with the parameters $\alpha(0) = 0.32$ and $T_B = 6$ GeV^2 that have been fixed in refs. [50,51]. To describe the energy dependence of the $\gamma p \to K^+ \Lambda$ differential cross-section at fixed t we have found $\gamma\nu = 2.75$.

We note in passing that logarithmic Regge trajectories have also been discussed in refs. [52–54]. The special limit $\gamma\nu \to 0$ at large $-t$ corresponds to "saturated" trajectories, *i.e.* all trajectories approach a constant asymptotically. Such a case leads to the "constituent-interchange model" that can be considered as a predecessor of the "asymptotic quark counting rules" [55,56]. Moreover, the model with "saturated" trajectories has also successfully been applied to the large-t behavior of exclusive photon- and hadron-induced reactions in refs. [48,57–59].

Formally, the amplitude (6) does not contain spin variables. Nevertheless, it can be used for a description of the differential cross-section that is averaged over the spin states of the initial particles and summed up over the polarizations of the final particles,

$$\frac{d\sigma_{\gamma p \to K^+ \Lambda}}{dt} = \frac{1}{64\pi s} \frac{1}{(p_\pi^{cm})^2}$$

$$\times \frac{1}{4} \sum_{\lambda_\gamma, \lambda_p, \lambda_\Lambda} \left| \langle \lambda_\Lambda | T_{\gamma p \to K^+ \Lambda}(s,t) | \lambda_p, \lambda_\gamma \rangle \right|^2 . \qquad (10)$$
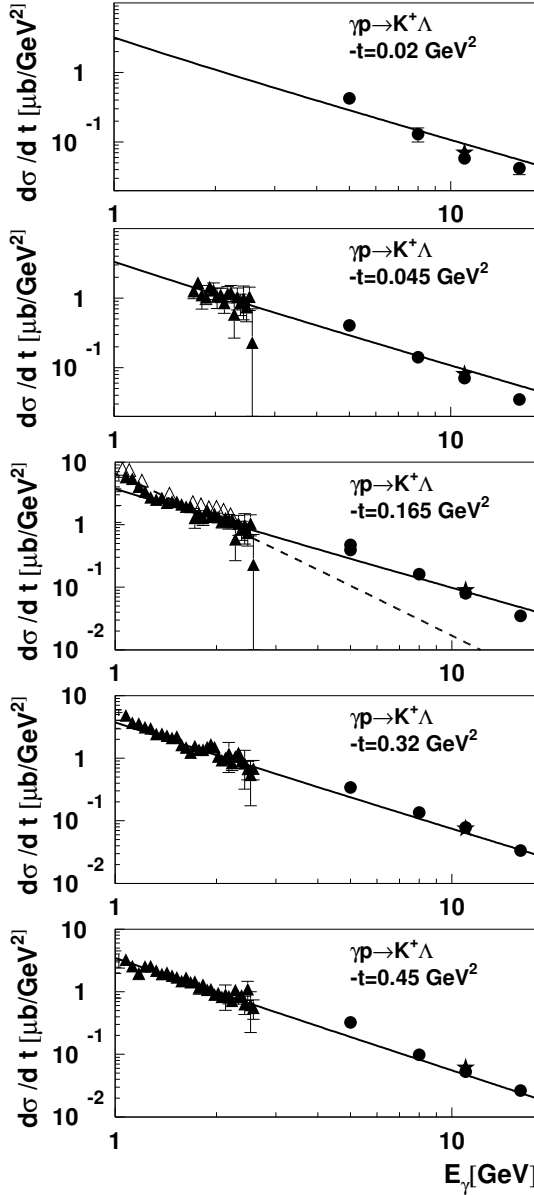
Fig. 3. Differential cross-section of the reaction $\gamma p \to K^+ \Lambda$ at $t = -0.02, -0.045, -0.165, -0.32$ and -0.45 GeV^2 as a function of the laboratory photon energy. The experimental data are from refs. [24] (full triangles), [62] (full circles), [63] (full stars), and [64] (empty triangles). The solid line is the result of the QGSM for the contribution of the K^* logarithmic Regge trajectory defined by eq. (9). The dashed line (for $t = -0.165$ GeV^2) describes the result for the K Regge trajectory $\alpha_K(t) = 0.7(t - m_K^2)$ normalized to the data of ref. [24] at $E_\gamma = 2$ GeV.

Here the amplitude squared can be written as

$$
\frac{1}{4} \sum_{\lambda_\gamma, \lambda_p, \lambda_\Lambda} \left| \langle \lambda_\Lambda | T_{\gamma p \to K^+ \Lambda}(s,t) | \lambda_p, \lambda_\gamma \rangle \right|^2 =
$$

$$
\frac{e^2}{4\gamma_\rho^2} g_{\rho KK^*}^2 \, g_{pK^*\Lambda}^2 |F_1(t)|^2 \left| -s/s_0^{K\Lambda} \right|^{2\alpha_{K^*}(t)} . \tag{11}
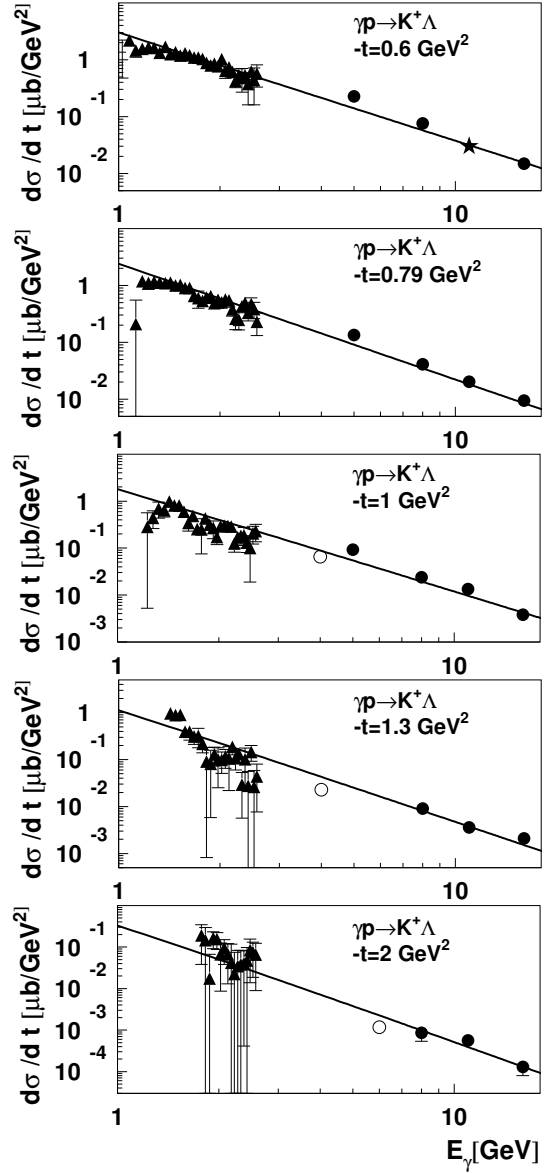$$

Fig. 4. Differential cross-section of the reaction $\gamma p \to K^+ \Lambda$ at $t = -0.6, -0.79, -1.0, -1.3$ and -2.0 GeV^2 as a function of the laboratory photon energy. The experimental data are from refs. [24] (full triangles), [62] (full circles), [63] (full stars), and [65] (empty circle). The solid lines are the results of the QGSM for the contribution of the K^* logarithmic Regge trajectory defined by eq. (9).

Let us now discuss constraints that have to be fulfilled for the residues and coupling constants. In line with refs. [34, 50, 60] we assume that for the planar quark diagrams with light quarks there is some kind of "universality" of the secondary Reggeon couplings to $q\bar{q}$-mesons involved in a binary reaction, *i.e.* in particular

$$
g_{\rho KK^*} \simeq g_{\pi KK^*} \simeq g_{\rho \pi \pi} = g_0 \tag{12}
$$

with $g_0 \simeq 5.8$. Taking $g_{\rho KK^*} = 5.8$ and normalising the differential cross-section of the reaction $\gamma p \to K^+ \Lambda$ at $t = 0$ we find $g_{pK^*\Lambda} \simeq 3.5$. This result shows that the

Reggeon couplings to mesons and baryons might be, in general, different by up to a factor of 2.

We mention that the form factor F_i —determining the t-dependence of the residue— was parametrized in refs. [34,50] as

$$F_i(t) = \Gamma(1 - \alpha_i(t)). \tag{13}$$

Indeed, such a choice of the form factor is convenient for an analytical continuation of the amplitude to positive t where the Γ function decreases exponentially with t. However, in the region of negative t the parametrization (13) exhibits a factorial growth and is not acceptable (see, *e.g.*, the discussion in ref. [61]). Accordingly we use the parametrization of the form factor (8), which decreases with t. To keep the same normalization of the amplitude at $t = 0$ we have to change the coupling constant squared as

$$g_0^2 \to g_M^2 = g_0^2 \Gamma(1 - \alpha_i(0)), \tag{14}$$

where for the K^* trajectory we have $\Gamma(1-\alpha_{K^*}(0)) \simeq 1.32$.

The differential cross-section for the reaction $\gamma p \to K^+\Lambda$ is presented in figs. 3, 4 as a function of the laboratory photon energy at fixed values of t. The solid lines are calculated using our model with the following coupling constants and parameters of the form factor: $g_{\rho K K^*} = 5.8$, $g_{pK^*\Lambda} \simeq 3.5$, $B_1 = 5$ GeV^{-2}, $R_1^2 = 1.13$ GeV^{-2}. The experimental data are from refs. [24] (full triangles), [62] (full circles), [63] (full stars), [64] (empty triangles) and [65] (empty circles). The agreement between the solid curves and the experimental data clearly supports the dominant role of the K^* Regge trajectory in the reaction $\gamma p \to K^+\Lambda$. The dashed line in fig. 3 —calculated at $t = -0.165$ GeV^2— describes the result for a K Regge trajectory normalized to the data at $E_\gamma = 2$ GeV. Definitely, it cannot describe the energy dependence of the differential cross-section and we may conclude that the K Regge trajectory is subdominant.

We have applied our model also to the description of the reaction $\gamma p \to K^+\Sigma^0$ adopting the same coupling constants and form factor as for the reaction $\gamma p \to K^+\Lambda$, however, modifying the scaling factor to $s_0^{K\Sigma} = (M_\Sigma + m_K)^2$. The total cross-sections of the reactions $\gamma p \to K^+\Lambda$ and $\gamma p \to K^+\Sigma^0$ as a function of the laboratory photon energy are shown in fig. 5 (the upper and lower parts describe the reactions $\gamma p \to K^+\Lambda$ and $\gamma p \to K^+\Sigma^0$, respectively) in comparison to the experimental data from ref. [24]. In this context one has to note that the Regge model gives only the average cross-section for a particular channel and misses resonant amplitudes at low energy. For example, according to recent data on the reaction $\gamma p \to K^+\Sigma^0$ [66], the s-channel resonance contributions are found to be important for photon beam energies at least up to 1.5 GeV. Since the $K^+\Lambda$ and $K^+\Sigma^0$ systems show strong resonances in the 1.3 to 2 GeV invariant-mass region, the latter cannot be described in the Regge approach. Nevertheless, the results of our model calculations (presented as the solid lines) are in good agreement with the data —except for the resonance structures mentioned above— and support the "universality" of Reggeon couplings.
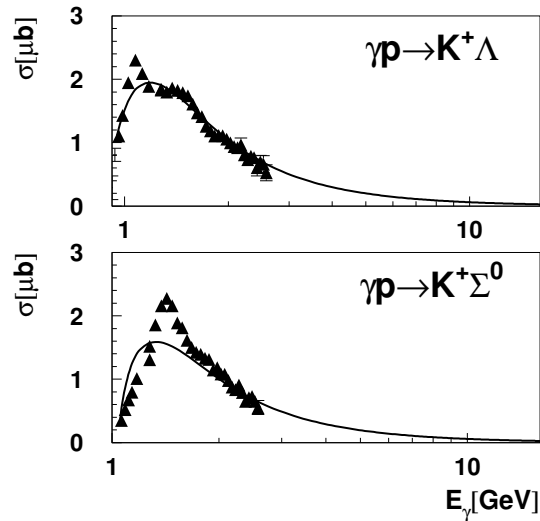

Fig. 5. Total cross-section of the reactions $\gamma p \to K^+\Lambda$ and $\gamma p \to K^+\Sigma^0$ as a function of the laboratory photon energy in comparison to the experimental data from [24]. The solid line is the result of the QGSM for the contribution of the K^* logarithmic Regge trajectory defined by eq. (9).
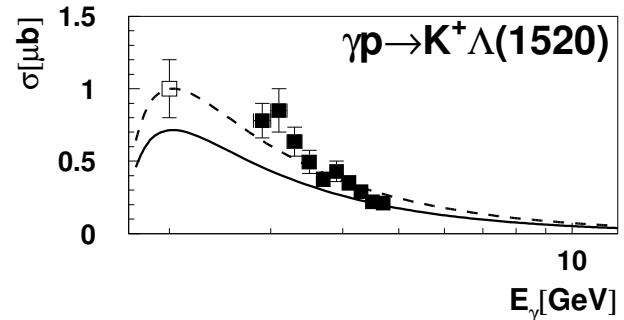

Fig. 6. Total cross-section of the reaction $\gamma p \to K^+\Lambda(1520)$ as a function of the laboratory photon energy in comparison to the experimental data from ref. [67] (full squares) and ref. [4] (open square). The solid line is the result of the QGSM for the contribution of the K^* logarithmic Regge trajectory defined by eq. (9) (see text); the dashed line results for a coupling $g_{pK^*Y} = 4.14$.

3 Total cross-sections for the reactions $\gamma p \to K^+\Lambda(1520)$ and $\gamma p \to \bar{K}^0\Theta^+$

In this section we explore if the universality of the K^* trajectory coupling to baryons with constituent qqs-quarks also holds in the binary reactions

$$\gamma p \to K^+ Y_i \tag{15}$$

with $Y_1 = \Lambda(1116), Y_2 = \Lambda(1520), \ldots$. In case of the universality to hold we have

$$g_{pK^*\Lambda(1520)} = g_{pK^*\Lambda} \simeq 3.5, \ F_{\Lambda(1520)}(t) = F_1(t). \tag{16}$$

The resulting total cross-section of the reaction $\gamma p \to K^+\Lambda(1520)$ is presented in fig. 6 in comparison to the experimental data from [67] (full squares) and [4] (empty
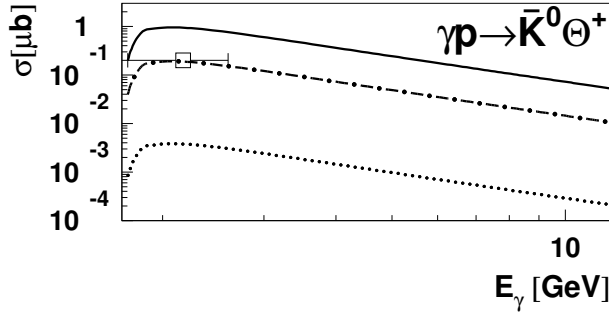
Fig. 7. Total cross-section of the reaction $\gamma p \to \bar{K}^0 \Theta^+$. The solid line results when assuming the validity of the universality principle also for the Θ^+ baryon. The dash-dotted curve is calculated for the reduced couplings (19) assuming the validity of the quoted cross-section (17). The dotted curve is calculated using the coupling constant $g_{pK^*\Theta}^{\text{CLAS}}$ (21) that corresponds to the preliminary upper limit from the CLAS Collaboration (20) on the total cross-section of the reaction $\gamma p \to \bar{K}^0 \Theta^+$ [68]. In the latter case the "universality principle" is found to be violated by almost 3 orders of magnitude.

square). The solid curve is calculated for the coupling constant $g_{pK^*Y} = 3.5$ which corresponds directly to the prediction from the universality principle. The dashed curve is calculated using $g_{pK^*Y} = 4.14$ and is in good agreement with the data; the deviation between the two curves does not exceed 40%. Therefore, the data on the reactions $\gamma p \to K^+ \Lambda$ and $\gamma p \to K^+ \Lambda(1520)$ support the assumption on the universality of the K^* trajectory coupling to $q\bar{q}$-mesons as well as to baryons with constituent qqs-quarks (at least within a factor of 2). We, accordingly, consider (or define) the universality principle to hold if a variety of cross-sections is described (predicted) within a factor better than 2.

We continue with the $\gamma p \to \bar{K}^0 \Theta^+$ reaction and explore if the unversality principle (in the sense defined above) also holds in this case. The cross-section of the reaction $\gamma p \to \bar{K}^0 \Theta^+$ was estimated by the SAPHIR Collaboration [4] as

$$\sigma_{\gamma p \to \bar{K}^0 \Theta^+} \simeq 200 \text{ nb} \qquad (17)$$

at an average photon energy of ~ 2 GeV. Let us first adopt 200 nb as an upper limit for the total cross-section of the reaction $\gamma p \to \bar{K}^0 \Theta^+$ at 2 GeV. In this case, eq. (17) implies already a noticeable violation of the universality principle for Θ^+ photoproduction since —assuming the universality principle to hold for Θ^+— we get

$$g_{pK^*\Theta} = g_{pK^*\Lambda(1520)} \simeq 4.14, \quad F_2(t) = F_1(t). \qquad (18)$$

This leads to a total cross-section of the reaction $\gamma p \to \bar{K}^0 \Theta^+$ shown by the solid line in fig. 7. The dash-dotted curve in fig. 7 is calculated assuming

$$g_{pK^*\Theta}^{\text{SAPHIR}} \simeq 0.4\, g_{pK^*\Lambda(1520)} \simeq 1.8 \,, \quad F_2(t) = F_1(t) \qquad (19)$$

in order to match the quoted cross-section (17). However, the new preliminary results from the CLAS Collaboration [68] do not support the estimate (17) and indicate
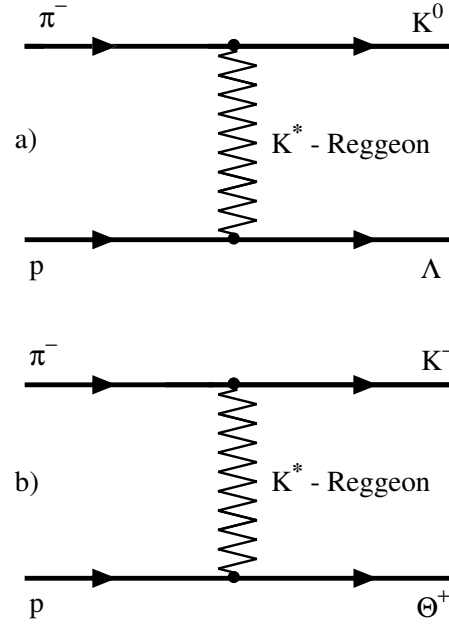

Fig. 8. K^*-Reggeon exchanges corresponding to the quark diagrams of fig. 1.

that the upper limit on the total cross-section of the reaction $\gamma p \to \bar{K}^0 \Theta^+$ should be much lower:

$$\sigma_{\gamma p \to \bar{K}^0 \Theta^+} \leq 1\text{–}4 \text{ nb} \,. \qquad (20)$$

When taking 4 nb as an upper limit we find

$$g_{pK^*\Theta}^{\text{CLAS}} \simeq 0.06\, g_{pK^*\Lambda(1520)} \simeq 0.25 \,, \quad F_2(t) = F_1(t) \,. \qquad (21)$$

Therefore, using the preliminary result from the CLAS Collaboration we find a very strong suppression of the $\gamma p \to \bar{K}^0 \Theta^+$ cross-section relative to the prediction from the universality principle for photoproduction of the lowest qqs baryons. If the pentaquark exists, we may interpret this finding as a clear indication of a substantially different quark structure of the Θ^+.

4 Pion-induced reactions: $\pi^- p \to K^0 \Lambda$ and $\pi^- p \to K^- \Theta^+$

We continue with π^--induced reactions and assume that the amplitudes of the reactions $\pi^- p \to K^0 \Lambda$ and $\pi^- p \to K^- \Theta^+$ are also dominated by the contribution of the K^* Regge trajectory (see fig. 8a) and b)) such that the cross-sections are fully determined. We directly step on with the results for the differential cross-section of the $\pi^- p \to K^0 \Lambda$ reaction as a function of t at $p_{\text{lab}} = 4.5, 6, 8, 10.7$ and 15.7 GeV/c shown in fig. 9 in comparison to the experimental data from [69,70]. The results of our model are displayed by the dashed lines calculated for the following parameters:

$$g_{\pi K^* K} = 5.8, \ g_{pK^*\Lambda} \simeq 4.5, \ B = 0, \ R_1^2 = 2.13 \text{ GeV}^{-2}. \qquad (22)$$

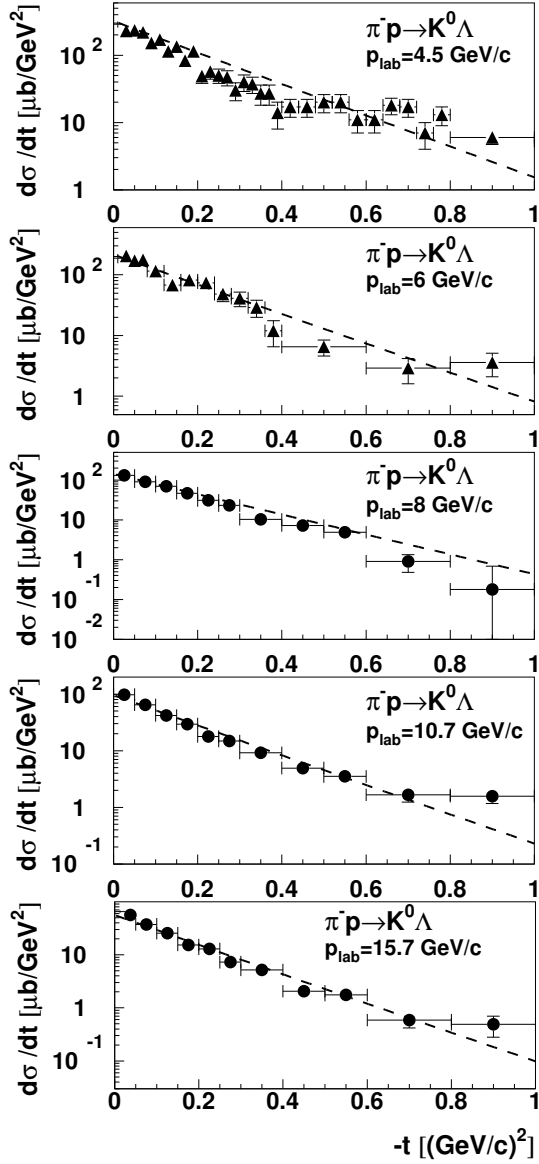**Fig. 9.** The differential cross-section of the $\pi^- p \to K^0 \Lambda$ reaction as a function of t at different laboratory momenta p_{lab} in comparison to the experimental data from [69] (full circles) and [70] (full triangles). The results of our model are shown by the dashed lines.

We see that the coupling constants $g_{\pi K^* K}$ and $g_{pK^* \Lambda}$ —in the case of the reaction $\pi^- p \to K^0 \Lambda$— are also in agreement with the universality assumption for the coupling constants. However, to describe the t-dependence of the differential cross-section we have to employ different parameters for the form factor $F(t)$ as compared to the reaction $\gamma p \to K^+ \Lambda$. This can be explained, in particular, by the different relative contributions of the baryon spin-flip terms in the reactions $\gamma p \to K^+ \Lambda$ and $\pi^- p \to K^0 \Lambda$.

The total cross-section of the reaction $\pi^- p \to K^0 \Lambda$ is presented in fig. 10, where the dashed curve is the result of our calculations. As expected for a Regge model —and discussed above— we see some deviation of the QGSM from the data [71] in the resonance region. However, at
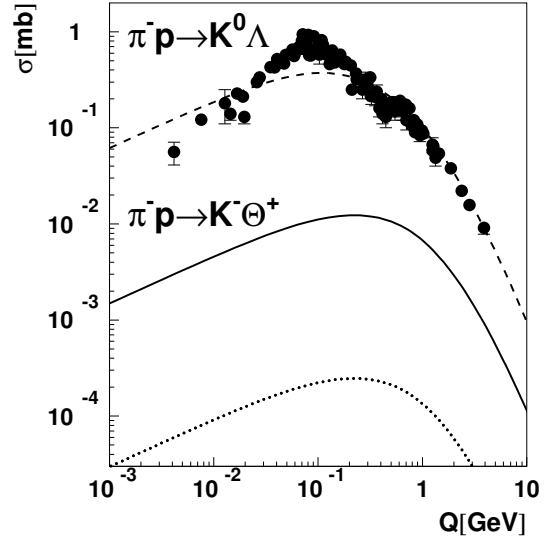

Fig. 10. Total cross-section of the reaction $\pi^- p \to K^0 \Lambda$ as a function of the c.m. excess energy $Q = \sqrt{s} - m_K - M_\Lambda$ (dashed line) in comparison to the data from ref. [71]. The solid and dotted line show the expected total cross-section of the reaction $\pi^- p \to K^- \Theta^+$ as a function of the c.m. excess energy $Q = \sqrt{s} - m_K - M_{\Theta^+(1540)}$ calculated with the coupling constants $g_{pK^*\Theta} = g_{pK^*\Theta}^{\text{SAPHIR}}$ (19) and $g_{pK^*\Theta}^{\text{CLAS}}$ (21).

higher energies, where the explicit resonance structure disappears, the theoretical calculations are in good agreement with the data.

Now using the coupling constants $g_{\pi K^* K} = 5.8$, $g_{pK^*\Theta} = g_{pK^*\Theta}^{\text{SAPHIR}}$ and $g_{pK^*\Theta}^{\text{CLAS}}$ and assuming R_1^2 and B to be the same as for the reaction $\pi^- p \to K^0 \Lambda$, we can calculate the cross-section for the reaction $\pi^- p \to K^- \Theta^+$. The results are shown in fig. 10 by the solid and dotted lines, respectively; these cross-sections reach about 10 (0.2) μb in their maximum.

5 Θ^+ production in exclusive and inclusive NN collisions

Further constraints on the universality of amplitudes and cross-sections for Θ^+ production are provided by NN collisions. Here the amplitude of the reaction $pp \to \Theta^+ \Sigma^+$ (cf. upper diagram in fig. 12 below) has been calculated using the coupling constant $g_{pK^*\Theta} = g_{pK^*\Theta}^{\text{SAPHIR}}$ ($g_{pK^*\Theta}^{\text{CLAS}}$). Of course, taking into account the results of sect. 2 we can safely assume that $g_{pK^*\Sigma} \simeq g_{pK^*\Lambda}$. At the same time the coupling constant $g_{pK^*\Lambda}$ may vary from 3.5 (if we define it via the reaction $\gamma p \to K^+ \Lambda$) to 4.5 (if we define it via the $\pi^- p \to K^0 \Lambda$ reaction). In this section we use $g_{pK^*\Lambda} = 4.5$. The predictions for the total cross-section of the $pp \to \Theta^+ \Sigma^+$ reaction are shown by the solid (dotted) line in fig. 11 using $g_{pK^*\Theta} = g_{pK^*\Theta}^{\text{SAPHIR}}$ ($g_{pK^*\Theta}^{\text{CLAS}}$). The cross-section described by the dotted line is $\sim$ 20–30 times smaller than the experimental value $\sigma = 0.4 \pm 0.1(\text{stat}) \pm 0.1(\text{syst})$ μb [11] measured at a beam momentum of 2.95 GeV/c (open square) and clearly signals an incompatibility of the different measurements.
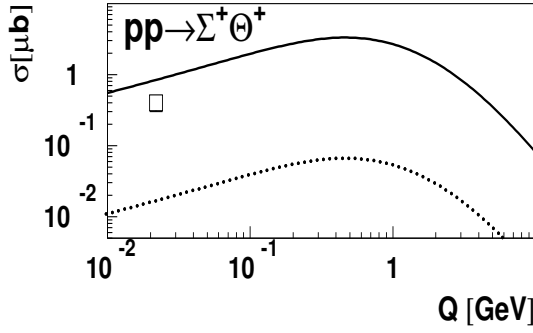
Fig. 11. Total cross-section for Θ^+ production as a function of the excess energy Q in the reaction $pp \to \Theta^+ \Sigma^+$. The solid (dotted) line is the result of a calculation with the coupling constants $g_{pK^*\Sigma} = g_{pK^*\Lambda} = 4.5$, $g_{pK^*\Theta} = g_{pK^*\Theta}^{\mathrm{SAPHIR}}$ ($g_{pK^*\Theta}^{\mathrm{CLAS}}$). The data point (open square) is from the COSY-TOF Collaboration [11].

We note that the first analysis of the reaction $pp \to \Theta^+ \Sigma^+$ was performed by Polyakov *et al.* in ref. [72] even before the Θ^+ baryon was "discovered" from the experimental side. Their estimation of the cross-section —within the kaon-exchange approximation— was about $2\,\mu$b at the initial momentum ~ 3 GeV/c. Approximately the same value of the total cross-section of the reaction $pp \to \Theta^+ \Sigma^+$ was found by Liu and Ko in ref. [73] later on. Our calculated cross-section is about $0.8\,\mu$b on the basis of the coupling (19) and 16 nb for the coupling (21) at the excess energy $Q = 22$ MeV ($p_{\mathrm{lab}} = 2.95$ GeV/c). The maxima of cross-sections are $3.3\,\mu$b and 66 nb, respectively, at the excess energy $Q = 460$ MeV ($p_{\mathrm{lab}} = 4.4$ GeV/c). These cross-sections are smaller by factors of 2 and 90, respectively, compared to the early estimates.

We continue with alternative production mechanisms for Θ^+ production in pp collisions as described by the middle and lower diagrams in fig. 12. In the following we use the method of Yao [74] to calculate the cross-sections of the reactions:

1) $pp \to p\bar{K}^0\Theta^+$ with the pion exchange (middle diagram in fig. 12),
2) $pp \to p\bar{K}^0\Theta^+$ with the kaon exchange (lower diagram in fig. 12 with $X = \bar{K}^0 p$),
3) $pp \to \Theta^+ X$ with the kaon exchange (lower diagram in fig. 12).

In the case of pion exchange the expression for the total cross-section can be written in the form

$$
\sigma(pp \to p\bar{K}^0\Theta^+) =
$$
$$
\frac{G_{\pi NN}^2}{8\pi^2 p_1^2 s} \int_{W_{\min}}^{W_{\max}} k\, W^2\, \sigma(\pi^0 p \to \bar{K}^0\Theta^+, W)\, \mathrm{d}W
$$
$$
\times \int_{t_{\min}(W)}^{t_{\max}(W)} F_\pi^4(t)\, \frac{1}{(t - m_\pi^2)^2}\, t\, \mathrm{d}t\,,
\tag{23}
$$

where W is the invariant mass of the $\bar{K}^0\Theta^+$ system, k is defined as

$$
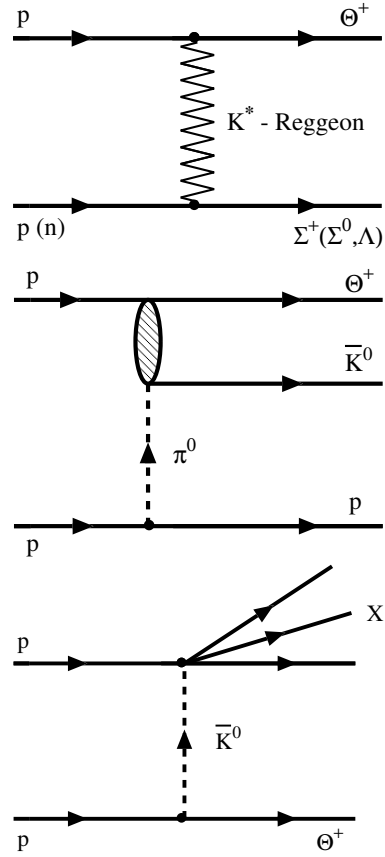k = \left((W^2 - (m_p - m_\pi)^2)(W^2 - (m_p + m_\pi)^2)\right)^{1/2}/2W\,,
$$

Fig. 12. The diagrams describing the Θ^+ production in the reactions: $pp \to \Theta^+ \Sigma^+$ or $pn \to \Theta^+ \Sigma^0(\Lambda)$ (upper diagram), $pp \to \Theta^+ \bar{K}^0 p$ with pion exchange (middle diagram) and $pp \to \Theta^+ X$ with kaon exchange (lower diagram).

p_1 is the initial proton momentum in the c.m. system, $t = (p_2 - p_4)^2$, and $G_{\pi NN} = 13.45$. Assuming that $J^P(\Theta^+) = \frac{1}{2}^+$ we have the following expression for the kaon-exchange contribution:

$$
\sigma(pp \to \Theta^+ X) =
$$
$$
\frac{G_{\Theta KN}^2}{8\pi^2 p_1^2 s} \int_{W_{\min}}^{W_{\max}} k\, W^2\, \sigma(\bar{K}^0 p \to X, W)\, \mathrm{d}W
$$
$$
\times \int_{t_{\min}(W)}^{t_{\max}(W)} F_K^4(t)\, \frac{1}{(t - m_K^2)^2}\, \left(t - \Delta_{M43}^2\right)\, \mathrm{d}t\,.
\tag{24}
$$

Here W is the invariant mass of the system X and $\Delta_{M43}^2 = (m_\Theta - m_p)^2$. The form factors for the virtual pion and kaon exchange have been chosen of the monopole type,

$$
F_j(t) = \frac{\Lambda_j^2 - m_j^2}{\Lambda_j^2 - t}\,,
\tag{25}
$$

with $\Lambda_\pi = 1.3$ GeV and $\Lambda_K = 1$ GeV. These parameters have been used in ref. [75] to describe the total cross-section of the reaction $pp \to K^+\Lambda p$. Obviously, the contribution of the kaon exchange to the reaction $pp \to \Theta^+ X$ depends on the coupling constant $G_{\Theta KN}$, which can only be estimated (or fixed by upper limits). If the Θ^+ decay width is less than 1 MeV [76] we have $G_{\Theta KN} \leq 1.4$.
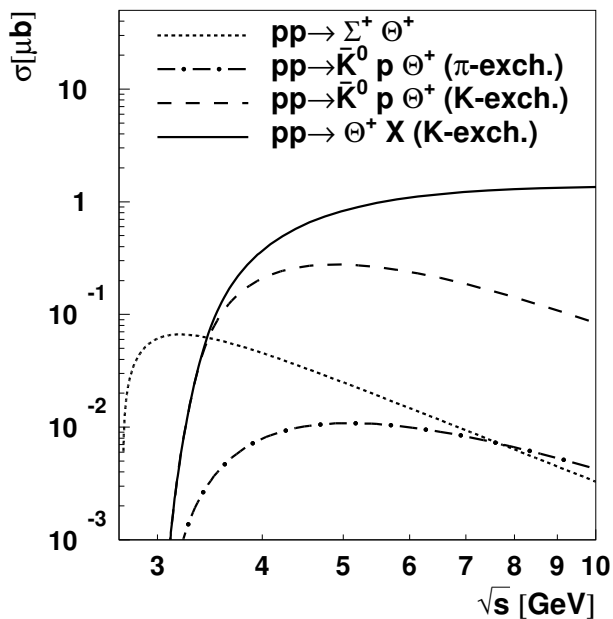
Fig. 13. Total cross-sections for Θ^+ production as a function of the c.m. energy in the reactions: $pp \to \Theta^+ \Sigma^+$ (dotted curve) and $pp \to \Theta^+ \bar{K}^0 p$ with pion exchange (dash-dotted line) calculated with the coupling constant $g_{pK^*\Theta} = g_{pK^*\Theta}^{\text{CLAS}}$ from eq. (21), $pp \to \Theta^+ \bar{K}^0 p$ with kaon exchange (dashed line), and $pp \to \Theta^+ X$ with kaon exchange (solid line).

The solid and dashed lines in fig. 13 present our results for the inclusive $pp \to \Theta^+ X$ and exclusive $pp \to \Theta^+ \bar{K}^0 p$ reactions as calculated within the kaon-exchange model for $G_{\Theta KN} = 1.4$ (as an upper limit). The inclusive cross-section turns out to be about 1.5 μb at high energies, while the exclusive $pp \to \Theta^+ \bar{K}^0 p$ cross-section is at least one order of magnitude smaller.

The reaction $pp \to p\bar{K}^0\Theta^+$ may proceed also via π exchange. The corresponding contribution to the total cross-section calculated with the coupling constant $g_{pK^*\Theta} = g_{pK^*\Theta}^{\text{CLAS}}$ from eq. (21) is presented by the dash-dotted line in fig. 13. It reaches about 10 nb in its maximum. Therefore, we can conclude that the Θ^+ production cross-section in pp collisions is dominated by the K exchange and should be about a few μb. Note that using the hadronic Lagrangian model, Liu and Ko [73] found a considerably larger cross-section for Θ^+ production, *i.e.* about 50 μb in pion-nucleon reactions and ~ 20 μb in proton-proton reactions. From our point of view the latter results are essentially due to a large coupling constant $G_{\Theta KN} \simeq 4.4$ in [73], which corresponds to $\Gamma_\Theta \approx 20$ MeV. Such large couplings, however, should be excluded according to the more recent analysis in ref. [77].

6 Conclusions

In this study we have analyzed Λ, Σ^0, $\Lambda(1520)$ and Θ^+ production in binary reactions induced by photon, pion and proton beams in the framework of the Quark-Gluon Strings Model combined with Regge phenomenology. Starting with the existing experimental data on the

$\gamma p \to K^+ \Lambda$ reaction, we have demonstrated that the differential and total cross-sections at photon energies 1–16 GeV and $-t < 2$ GeV^2 can be described very well by the model with a dominant contribution of the K^* Regge trajectory. We stress that the rather good description of the large-t region was possible only due to the logarithmic form of the K^* Regge trajectory (9). It has been demonstrated, furthermore, that the data on the reactions $\gamma p \to K^+ \Lambda$, $\gamma p \to K^+ \Sigma^0$ and $\gamma p \to K^+ \Lambda(1520)$ —at least within a factor of 2— support the assumption on the universality of the K^* trajectory coupling to $q\bar{q}$-mesons as well as to baryons with qqs constituent quarks. This implies that —using the same parameters as for $\gamma p \to K^+ \Lambda$— we are able to reproduce the total $\gamma p \to K^+ \Sigma^0$ and $\gamma p \to K^+ \Lambda(1520)$ cross-sections (within an accuracy of 40%). On the other hand, as a consequence of the SAPHIR data [4] and the preliminary data from CLAS [68], there is an essential suppression of the $\gamma p \to \bar{K}^0\Theta^+$ cross-section relative to the prediction within the universality principle that was shown to hold (with reasonable accuracy) for the photoproduction of the lowest qqs-baryons. We conclude that this suppression indicates a substantially different quark structure and wave function of the Θ^+ (in case of its final experimental confirmation).

Moreover, we have suggested that the amplitudes of the reactions $\pi^- p \to K^0 \Lambda$ and $\pi^- p \to K^- \Theta^+$ are also dominated by the contribution of the K^* Regge trajectory (cf. fig. 8a) and b)). Indeed, the differential and total cross-sections of the $\pi^- p \to K^0 \Lambda$ reaction are found to be in reasonable agreement with the universality principle. Using parameters defined by the analysis of the reactions $\gamma p \to K^+ \Lambda$, $\gamma p \to K^+ \Sigma^0$, $\gamma p \to K^+ \Lambda(1520)$, $\gamma p \to \bar{K}^0\Theta^+$ and $\pi^- p \to K^0 \Lambda$, we have calculated the cross-section for the reaction $\pi^- p \to K^- \Theta^+$. We predicted a maximum cross-section of about 200 nb (cf. fig. 10) for the coupling constant $g_{pK^*\Theta} = g_{pK^*\Theta}^{\text{CLAS}}$ extracted from the new preliminary CLAS result on the reaction $\gamma p \to \bar{K}^0\Theta^+$ [68].

We extended our model additionally to the analysis of the binary reaction $pp \to \Sigma^+\Theta^+$. We found that the cross-section of this reaction —measured by the COSY-TOF Collaboration [11]— is 20–30 times larger than the value predicted by the model with the coupling constant $g_{pK^*\Theta} = g_{pK^*\Theta}^{\text{CLAS}}$. Furthermore, we have investigated the exclusive and inclusive Θ^+ production in the reactions $pp \to p\bar{K}^0\Theta^+$ and $pp \to \Theta^+ X$ and found that the inclusive Θ^+ production in pp collisions at high energy should be on the level of 1 μb.

The systematic and comparative Regge analysis —provided by our study— will also allow in the future to relate different data sets from γ-, π- and proton-induced reactions on $s\bar{s}$ pair production and finally should yield a transparent picture of the dynamics as well as the properties of (possible) exotic states.

References

1. LEPS Colaboration (T. Nakano *et al.*), Phys. Rev. Lett. **91**, 012002 (2003).
2. DIANA Collaboration (V.V. Barmin *et al.*), Phys. At. Nucl. **66**, 1715 (2003).
3. CLAS Collaboration (S. Stepanyan *et al.*), Phys. Rev. Lett. **91**, 252001 (2003).
4. SAPHIR Collaboration (J. Barth *et al.*), Phys. Lett. B **572**, 127 (2003), hep-exp/0307083.
5. HERMES Collaboration (A. Airapetian *et al.*), Phys. Lett. B **585**, 213 (2004).
6. V. Kubarovsky *et al.*, AIP Conf. Proc. **698**, 543 (2004).
7. A.E. Asratyan, A.G. Dolgolenko, M.A. Kubantsev, Phys. At. Nucl. **67**, 682 (2004).
8. NA49 Collaboration (C. Alt *et al.*.), Phys. Rev. Lett. **92**, 042003, (2004).
9. CLAS Collaboration (V. Kubarovsky *et al.*), Phys. Rev. Lett. **92**, 032001 (2004); **92**, 049902 (2004)(E).
10. SVD Collaboration (A. Aleev *et al.*), hep-exp/0401024.
11. COSY-TOF Collaboration (M. Abdel-Bary *et al.*), Phys. Lett. B **595**, 127 (2004).
12. D. Diakonov, V. Petrov, M. Polyakov, Z. Phys. A **359**, 305 (1997).
13. R.L. Jaffe, F. Wilczek, Phys. Rev. Lett. **91**, 232003 (2003); M. Karliner, H.J. Lipkin, hep-ph/0307243; Phys. Lett. B **575**, 249 (2003).
14. T. Hyodo, A. Hosaka, Phys. Rev. D **71**, 054017 (2005).
15. M. Oka, Prog. Theor. Phys. **112**, 1 (2004).
16. S.R. Beane, Phys. Rev. D **70**, 114010 (2004).
17. B.L. Ioffe, A.G. Oganesian, JETP Lett. **80**, 386 (2004).
18. R.L. Jaffe, Phys. Rep. **409**, 1 (2005).
19. J. Sugiyama, T. Doi, M. Oka, Phys. Lett. B **581**, 167 (2004).
20. F. Csikor, Z. Fodor, S.D. Katz, T.G. Kovacs, J. High Energy Phys. **0311**, 070 (2003).
21. G.S. Bali, nucl-th/0502046.
22. T.-W. Chiu, T.-H. Hsieh, hep-ph/0403020; S. Sasaki, Phys. Rev. Lett. **93**, 152001 (2004); hep-lat/0410016.
23. F. Csikor, Z. Fodor, S.D. Katz, T.G. Kovacs, B.C. Toth, hep-lat/0503012.
24. K.-H. Glander *et al.*, Eur. Phys. J. A **19**, 251 (2004).
25. C. Bochna *et al.*, Phys. Rev. Lett. **81**, 4576 (1998); E.C. Schulte *et al.*, Phys. Rev. Lett. **87**, 102302 (2001); E.C. Schulte *et al.*, Phys. Rev. C **66**, 042201(R) (2002); M. Mirazita *et al.*, Phys. Rev. C **70**, 014005 (2004).
26. Y. Oh, H.C. Kim, S.H. Lee, Phys. Rev. D **69**, 074016 (2004).
27. S.I. Nam, A.Hosaka, H.-Ch. Kim, Phys. Lett. B **579**, 43 (2004).
28. W.W. Li *et al.*, High Energy Phys. Nucl. Phys. **28**, 918 (2004).
29. P. Ko, J. Lee, T. Lee, J.H. Park, Phys. Lett. B **611**, 87 (2005).
30. W. Liu, C.M. Ko, V. Kubarovsky, Phys. Rev. C **69**, 025202 (2004).
31. B.G. Yu, T.K. Choi, C.R. Ji, Phys. Rev. C **70**, 045205 (2004).
32. T. Mart, Phys. Rev. C **71**, 022202 (2005).
33. A.B. Kaidalov, Z. Phys. C **12**, 63 (1982).
34. A.B. Kaidalov, Surv. High Energy Phys. **13**, 265 (1999).
35. A.B. Kaidalov, L.A. Kondratyuk, D.V. Tchekin, Phys. At. Nucl. **63**, 1395 (2000).
36. V.Yu. Grishina *et al.*, Eur. Phys. J. A **10**, 355 (2001).
37. V.Yu. Grishina *et al.*, Eur. Phys. J. A **19**, 117 (2004).
38. G. 't Hooft, Nucl. Phys. B **72**, 461 (1974).
39. G. Veneziano, Phys. Lett. B **52**, 220 (1974); Nucl. Phys. B **117**, 519 (1976).
40. A. Casher, J. Kogut, L. Susskind, Phys. Rev. D **10**, 732 (1974).
41. X. Artru, G. Mennesier, Nucl. Phys. B **70**, 93 (1974).
42. A. Casher, H. Neuberger, S. Nussinov, Phys. Rev. D **20**, 179 (1979).
43. B. Andersson, G. Gustafson, C. Peterson, Phys. Lett. B **71**, 337 (1977); Z. Phys. C **1**, 105 (1979).
44. E.G. Gurvich, Phys. Lett. B **87**, 386 (1979).
45. K.G. Boreskov, A.B. Kaidalov, Sov. J. Nucl. Phys. **37**, 100 (1983).
46. A.C. Irving, R.P. Worden, Phys. Rep. **34**, 117 (1977).
47. N. Levy, W. Majerotto, B.W. Read, Nucl. Phys. **55**, 493 (1973).
48. M. Guidal, J.M. Laget, M. Vanderhaeghen, Nucl. Phys. A **627**, 645 (1997).
49. D.D. Coon *et al.*, Phys. Rev. D **18** , 1451 (1978).
50. A.B. Kaidalov, P.E. Volkovitsky, Z. Phys. C **63**, 517 (1994).
51. M.M. Brisudová, L. Burakovsky, T. Goldman, Phys. Rev. D **61** , 054013 (2000).
52. A.I. Bugrij, G. Cohen-Tannoudji, L.L. Jenkovszky, N.I. Kobylinsky, Fortschr. Phys. **31** , 427 (1973).
53. H. Ito, Prog. Theor. Phys. **84** , 94 (1990).
54. Z.E. Chikovani, L.L. Jenkovszky, F. Paccanoni, Mod. Phys. Lett. A **6**, 1409 (1991).
55. S.J. Brodsky, G.R. Farrar, Phys. Rev. Lett. **31**, 1153 (1973); V. Matveev, R.M. Muradyan, A.N. Tavkhelidze. Lett. Nuovo Cimento **7**, 719 (1973).
56. S.J. Brodsky, J.R. Hiller, Phys. Rev. C **28**, 475 (1983).
57. R. Fiore *et al.*, Phys. Rev. D **60**, 116003 (1999).
58. C. White *et al.*, Phys. Rev. D **49**, 58 (1994).
59. M. Battaglieri *et al.*, Phys. Rev. Lett. **87**, 172002 (2001).
60. A.B. Kaidalov, A.V. Nogteva, Sov. J. Nucl. Phys. **47**, 321 (1988).
61. W. Cassing, L.A. Kondratyuk, G.I. Lykasov, M.V. Rzjanin, Phys. Lett. B **513**, 1 (2001).
62. A.M. Boyarski *et al.* Phys. Rev. Lett. **22**, 1131 (1969).
63. A.M. Boyarski *et al.* Phys. Lett. B **34**, 547 (1971).
64. P. Feller *et al*, Nucl. Phys. B **39**, 413 (1972).
65. R.L. Anderson *et al.* Phys. Rev. D **14**, 679 (1976).
66. J.W.C. McNabb *et al.* Phys. Rev. C **69**, 042201 (2004).
67. D.P. Barber *et al.*, Z. Phys. C **7**, 17 (1980).
68. M. Battaglieri, R. De Vita, V. Kubarovsky, D. Weygand, the CLAS Collaboration, interactive: http//clasweb.jlab.org/csc.
69. K.J. Foley *et al.*, Phys. Rev. D **8**, 27 (1973).
70. D.J. Crennell *et al.*, Phys. Rev. D **6**, 1220 (1972).
71. H. Schopper (Editor), *Landoldt-Börnstein, New Series*, Vol. **I/12** (Springer, Berlin, 1988).
72. M.V. Polyakov *et al.*, Eur. Phys. J. A **9**, 115 (2000).
73. W. Liu, C.M. Ko, Phys. Rev. C **68**, 045203 (2003).
74. T. Yao, Phys. Rev. **125**, 1048 (1962).
75. A.M. Gasparyan *et al.*, Eur. Phys. J. A **18**, 305 (2003).
76. Particle Data Group (S. Eidelman *et al.*), Phys. Lett. B **592**, 1 (2004).
77. A. Sibirtsev, J. Haidenbauer, S. Krewald, Ulf-G. Meissner, Eur. Phys. J. A **23**, 491 (2005); Phys. Lett. B **599**, 230 (2004).